Inorg. Chem. **2008**, *47*, 11423−11428

Electrochemical and Spectroscopic Characterization of a Series of Mixed-Ligand Diruthenium Compounds

Karl M. Kadish,*,† Rachel Garcia,† Tuan Phan,‡ Julien Wellhoff,† Eric Van Caemelbecke,†,§ and John L. Bear*,†

Department of Chemistry, University of Houston, Houston, Texas 77204-5003, Department of Chemistry, Texas Southern University, Houston, Texas 77004, and Houston Baptist University, 7502 Fondren Road, Houston, Texas 77074-3298

Received September 9, 2008

The electrochemistry and spectroelectrochemistry of a novel series of mixed-ligand diruthenium compounds were examined. The investigated compounds having the formula $Ru_2(CH_3CO_2)_x(Fap)_{4-x}Cl$ where $x = 1-3$ and Fap is 2-(2-fluoroanilino)pyridinate anion were made from the reaction of $Ru_2(CH_3CO_2)_4Cl$ with 2-(2-fluoroanilino)pyridine (HFap) in refluxing methanol. The previously characterized $Ru_2(Fap)_4Cl$ as well as the three newly isolated compounds represented as $Ru_2(CH_3CO_2)(Fap)_3Cl$ (**1**), $Ru_2(CH_3CO_2)_2(Fap)_2Cl$ (**2**), and $Ru_2(CH_3CO_2)_3(Fap)Cl$ (**3**) possess three unpaired electrons with a Ru_2^{5+} dimetal core. Complexes **1** and **2** have well-defined $Ru_2^{5+/4+}$ and $Ru_2^{5+/6+}$ redox couples in CH_2Cl_2, but **3** exhibits a more complicated electrochemical behavior due to equilibria involving association or dissociation of the anionic chloride axial ligand on the initial and oxidized or reduced forms of the compound. The $E_{1/2}$ values for the $Ru_2^{5+/4+}$ and $Ru_2^{5+/6+}$ processes vary linearly with the number of $CH_3CO_2^-$ bridging ligands on $Ru_2(CH_3CO_2)_x(Fap)_{4-x}Cl$ and plots of reversible half-wave potentials vs the number of acetate groups follow linear free energy relationships with the largest substituent effect being observed for the oxidation. The major UV−visible band of the examined compounds in their neutral Ru_2^{5+} form is located between 550 and 800 nm in CH_2Cl_2 and also varies linearly with the number of $CH_3CO_2^-$ ligands on $Ru_2(CH_3CO_2)_x(Fap)_{4-x}Cl$. The electronic spectra of the singly oxidized and singly reduced forms of each diruthenium species were characterized by UV−visible spectroelectrochemistry in CH_2Cl_2.

Introduction

A number of Ru_2^{5+} complexes, with mixed acetate and other monoanionic bridging ligands, have been reported in the literature.[1−20] $Ru_2(mhp)_2(CH_3CO_2)_2Cl$ (Hmhp = 6-methyl-2-hydroxypyridine) was the first reported Ru_2^{5+} complex with mixed bridging ligands of this type and was obtained by reacting $Ru_2(CH_3CO_2)_4Cl$ with Hmhp in boiling methanol.[3] Other mixed-ligand diruthenium complexes were subsequently prepared by a variety of synthetic methods, two examples being $Ru_2(CH_3CO_2)_x(L)_{4-x}Cl$,[9,10] where $x = 0-3$ and L is formamidinate, a symmetrical N,N′ donor bridging ligand and $Ru_2(O_2CMe)_x(admp)_{4-x}Cl$,[4] where $x = 0-3$ and admp is the unsymmetrical bridging ligand, 2-amino-4,6-dimethylpyridinate. In the present paper we have synthesized a series of mixed-ligand Ru_2^{5+} complexes having the formula $Ru_2(CH_3CO_2)_x(Fap)_{4-x}Cl$ where $x = 1-3$ and Fap is an unsymmetrical 2-fluoroanilinopyridinate anion. The fully substituted and previously characterized $Ru_2(Fap)_4Cl$[21] was also produced in the reaction mixture.

One goal of this study was to monitor how $E_{1/2}$ values for generation of the Ru_2^{4+} or Ru_2^{6+} forms of the compounds vary as a function of the number of Fap^- or acetate bridging ligands and another was to monitor systematic changes in the UV−visible spectra for the compounds in their high and

* To whom correspondence should be addressed. E-mail: kkadish@uh.edu (K.M.K.), jbear@uh.edu (J.L.B.).
† University of Houston.
‡ Texas Southern University.
§ Houston Baptist University.

(1) Angaridis, P. *In Multiple Bonds Between Metal Atoms*, 3rd ed.; Cotton, F. A.; Murillo, C. A.; Walton, R. A., Eds.; Springer Science and Business Media Inc.: New York, **2005**; Chapter 9.
(2) Chakravarty, A. R.; Cotton, F. A. *Inorg. Chim. Acta* **1985**, *105*, 19.
(3) Chakravarty, A. R.; Cotton, F. A.; Tocher, D. A. *Inorg. Chem.* **1985**, *24*, 2857.
(4) Cotton, F. A.; Yokochi, A. *Inorg. Chem.* **1998**, *37*, 2723.
(5) McCarthy, H. J.; Tocher, D. A. *Polyhedron* **1992**, *11*, 13.
(6) Ren, T.; DeSilva, V.; Zou, G.; Lin, C.; Daniels, L. M.; Campana, C. F.; Alvarez, J. C. *Inorg. Chem. Commun.* **1999**, *2*, 301.

10.1021/ic8017369 CCC: $40.75 © 2008 American Chemical Society
Published on Web 11/05/2008

low oxidation states after generating the electrooxidized or electroreduced forms of the compound at a controlled potential in a thin-layer cell.

Experimental Section

Chemicals and Reagents. Ultra high purity nitrogen gas was purchased from Matheson Tri-Gas and was passed through a container filled with anhydrous calcium sulfate and potassium hydroxide pellets to remove traces of water and oxygen prior to use. Tetra-*n*-butylammonium perchlorate (TBAP), purchased from Fluka Chemical Co., was recrystallized from ethyl alcohol and stored in a vacuum oven at 40 °C for one week prior to use. Tetra-*n*-butylammonium chloride (TBACl) purchased from Fluka Chemical Co. was used without further purification. Dichloromethane DriSolv was purchased from EMD Scientific and was used without further purification. Silica gel (Merck 230−400 mesh 60 Å) was purchased from Sorbent Technologies and used as received. Acetone (ace), methanol, and hexanes were purchased from Sigma-Aldrich and were used without further purification.

Physical Measurements. Cyclic voltammetry was carried out using either an IBM model 225 potentiostat coupled with an EG&G XY plotter or a computer based EG&G potentiostat model 263A. A three-electrode system was used and consisted of a glassy carbon working electrode, a platinum counter electrode, and a homemade saturated calomel electrode (SCE) as the reference electrode. A fritted-glass bridge filled with the solvent and supporting electrolyte was used to separate the SCE from the bulk of the solution. The bulk solution was deaerated and the electrochemical measurement was recorded under a N_2 blanket. UV−visible spectroelectrochemistry was carried out using a homemade thin-layer cell whose design has been reported in the literature.[22] The UV−visible spectra were recorded with a Hewlett-Packard model 8453 diode array spectrophotometer. Mass spectra were recorded on a Finnigan TSQ 700 instrument at the University of Texas, Austin. A standard fast bombardment was used, and *m*-nitrobenzyl alcohol (NBA) was used as the liquid matrix.

Controlled-potential electrolyses were carried out with an EG&G model 173 potentiostat to electrogenerate the singly reduced Ru_2^{4+} forms of each compound for measurements of their magnetic moment using the Evans method.[23] The electroreduction was performed in a glovebag filled with an inert gas where 5 mg of the investigated complex was dissolved in 10 mL of CD_3CN. After complete electrolysis at potentials negative of $E_{1/2}$ for the $Ru_2^{5+/4+}$ process, 1 mL of the reduced solution was transferred and sealed in an NMR tube containing a few drops of deaerated TMS. Magnetic susceptibilities of the neutral compounds were also measured using the Evans method.[23] Elemental analysis was carried out by Atlantic Microlab Inc., Norcross Georgia.

Synthesis of Starting Materials. $Ru_2(CH_3CO_2)_4Cl$,[24,25] and 2-(2-fluoroanilino)pyridine (HFap),[21] were synthesized following methods described in the literature.

Synthesis of $Ru_2(CH_3CO_2)_x(Fap)_{4-x}Cl$ ($x = 0-3$). 200 mg (0.42 mmol) of $Ru_2(CH_3CO_2)_4Cl$ and 239 mg (1.26 mmol) of HFap were placed in a round-bottom flask equipped with a condenser and refluxed for 3 h in 15 mL of methanol under nitrogen. During this time, the solution changed from brown to blue-green. After completion of the reaction, the solvent was evaporated using a rotary evaporator. Ruthenium acetate was removed by vacuum filtration using a fritted disk filter and dichloromethane as solvent. The filtrate was evaporated to about 1 mL and the residue was analyzed on a TLC plate followed by separation on a silica column using 1:1-(v:v hexanes/acetone) as eluent. Four bands, two green, one blue, and one purple, were observed and collected. These bands had R_f values of 0.875, 0.825, 0.525 and 0.175 from the TLC and were identified as $Ru_2(Fap)_4Cl$ (**0**), $Ru_2(CH_3CO_2)(Fap)_3Cl$ (**1**), $Ru_2(CH_3CO_2)_2(Fap)_2Cl$ (**2**) and $Ru_2(CH_3CO_2)_3(Fap)Cl$ (**3**), respectively, on the basis of their mass spectral data and/or X-ray crystal structure. The percent yields were 14.9, 11.1, 41.0, and 29.3%, respectively. When the reaction was carried out under the same conditions for 6 instead of 3 h, the respective percent yields were 30.2, 20.1, 24.2, and 4.8%, respectively. Thus, changing the reaction time provided some control over the relative yields of each product in the series of compounds. A characterization of compound **0** was previously reported in the literature.[21]

$Ru_2(CH_3CO_2)(Fap)_3Cl$ (1). Mass spectral data [*m*/*z*, (fragment)]: 859 $[Ru_2(CH_3CO_2)(Fap)_3Cl]^+$, 824 $[Ru_2(CH_3CO_2)(Fap)_3]^+$, 799 $[Ru_2(Fap)_3]^+$. Anal. Calc. for $C_{35}H_{27}N_6O_2F_3Ru_2Cl$: C, 49.01; H, 3.16; N, 9.47. Found: C, 48.98; H, 3.17; N, 9.79. Magnetic moment: 4.01 μ_B at 297 K.

$Ru_2(CH_3CO_2)_2(Fap)_2Cl$ (2). Mass spectral data [*m*/*z*, (fragment)]: 731 $[Ru_2(CH_3CO_2)_2(Fap)_2Cl]^+$, 696 $[Ru_2(CH_3CO_2)_2(Fap)_2]^+$, 672 $[Ru_2(CH_3CO_2)(Fap)_2Cl]^+$. Anal. Calc. for $C_{26}H_{22}N_4O_4F_2Ru_2Cl$: C, 42.80; H, 3.03; N, 7.67. Found C, 42.77; H, 3.04; N, 7.67. Magnetic moment: 3.64 μ_B at 297 K.

$Ru_2(CH_3CO_2)_3(Fap)Cl$ (3). Mass spectral data [*m*/*z*, (fragment)]: 600 $[Ru_2(CH_3CO_2)_3(Fap)Cl]^+$, 567 $[Ru_2(CH_3CO_2)_3(Fap)]^+$. Anal. Calc. for $C_{17}H_{17}N_2O_6F_1Ru_2Cl$: C, 39.90; H, 3.84; N, 4.65. Found C, 40.24; H, 4.26; N, 4.65. Magnetic moment: 3.82 μ_B at 297 K.

X-ray Crystallography of $Ru_2(CH_3CO_2)_2(Fap)_2Cl$ (2). $Ru_2(CH_3CO_2)_2(Fap)_2Cl$ was dissolved in an acetone/hexanes mixture (7:3,v:v) and the solvent was slowly evaporated at room temperature to obtain a single crystal for X-ray analysis. Measurements were made with a Siemens SMART platform diffractometer using monochromated Mo Kα radiation and equipped with a 1 K CCD area detector. A hemisphere of data (1271 frames at 5 cm detector distance) was collected using a narrow-frame method with scan widths of 0.30 deg in omega and an exposure time of 35 s/frame. The first 50 frames were remeasured at the end of data collection

(7) Angaridis, P.; Berry, J. F.; Cotton, F. A.; Murillo, C. A.; Wang, X. *J. Am. Chem. Soc.* **2003**, *125*, 10327.
(8) Angaridis, P.; Berry, J. F.; Cotton, F. A.; Lei, P.; Lin, C.; Murillo, C. A.; Villagran, D. *Inorg. Chem. Commun.* **2004**, *7*, 9.
(9) Barral, M. C.; Herrero, S.; Jimenez-Aparicio, R.; Torres, M. R.; Urbanos, F. A. *Inorg. Chem. Commun.* **2004**, *7*, 42.
(10) Angaridis, P.; Cotton, F. A.; Murillo, C. A.; Villagran, D.; Wang, X. *Inorg. Chem.* **2004**, *43*, 8290.
(11) Collin, J.-P.; Jouaiti, A.; Sauvage, J.-P.; Kasha, W. C.; McLoughlin, M. A.; Keder, N. L.; Harrison, W. T. A.; Stucky, G. D. *Inorg. Chem.* **1990**, *29*, 2238.
(12) Mintvert, M.; Sheldrick, W. S. *Inorg. Chim. Acta* **1995**, *236*, 13.
(13) Kachi-Terajima, C.; Miyasaka, H.; Ishii, J. T.; Sugiura, K.; Yamashita, M. *Inorg. Chim. Acta* **2002**, *332*, 210.
(14) Miyasaka, H.; Kachi-Terajima, C.; Ishii, T.; Yamashita, M. J. *Chem. Soc. Dalton Trans.* **2001**, 1929.
(15) Miyasaka, H.; Izawa, T.; Sugiura, K.; Yamashita, M. *Inorg. Chem.* **2003**, *42*, 7683.
(16) Barral, M.; Herrero, S.; Jimenez-Aparicio, R.; Torres, M. R.; Urbanos, F. A. *J. Organomet. Chem.* **2008**, *693*, 1597.
(17) Barral, M.; Gallo, T.; Herrero, S.; Jimenez-Aparicio, R.; Torres, R.; Urbanos, F. A. *Chem. A. Eur. J.* **2007**, *13*, 10088.
(18) Chen, W.-Z.; Protasiewicz, J. D.; Davis, S. A.; Updegraff, J. B.; Ma, L.-Q.; Fanwick, E.; Ren, T. *Inorg. Chem.* **2007**, *46*, 3775.
(19) Chen, W. Z.; Protasiewicz, J. D.; Shirar, A. J.; Ren, T. *Eur. J. Inorg. Chem.* **2006**, *23*, 4737.
(20) Barral, M. C.; Gallo, T.; Herrero, S.; Jimenez-Aparacio, R.; Torres, M. R.; Urbanos, F. A. *Inorg. Chem.* **2006**, *45*, 3639.
(21) Bear, J. L.; Wellhoff, J.; Royal, G.; Van Caemelbecke, E.; Eapen, S.; Kadish, K. M. *Inorg. Chem.* **2001**, *40*, 2282.
(22) Lin, X. Q.; Kadish, K. M. *Anal. Chem.* **1985**, *57*, 1489.
(23) Evans, D. F. *J. Chem. Soc.* **1959**, 2003.
(24) Stephenson, T. A.; Wilkinson, G. *J. Inorg. Nucl. Chem.* **1966**, *28*, 2285.

Table 1. Crystallographic Data of $Ru_2(CH_3CO_2)_2(Fap)_2Cl(ace)$ **2**

formula	$Ru_2ClO_6N_4C_{32}H_{34}$
formula weight	846.22
crystal system	monoclinic
space group	*C*2/*c*
a, Å	19.666
b, Å	14.041
c, Å	25.487
α, degrees	90.0
β, degrees	104.18
γ, degrees	90.0
V, Å^3	6823
Z	8
D_{calc}, g/cm^3	1.65
crystal size, mm	0.35 × 0.30 × 0.08
μ(Mo Kα), cm^{-1}	10.23
data collection instrument	Siemens SMART platform diffractometer
radiation (monochromated In incident beam)	Mo (Kα = 0.71073)
temperature, K	223
data collection range, θ, deg.	1.80 to 23.53
total number of data	5307
with $F_o^2 > 3\sigma(F_o^2)$	5069
number of parameters refined	332
trans factors, max, min	88%, 70%
R^a	0.038
$R_w{}^b$	0.092
quality-of-fit indicator	1.04

^{a} $R = \Sigma||F_o| - |F_c||/\Sigma|F_o|$. ^{b} $R_w = [\Sigma_w(|F_o| - |F_c|)^2/\Sigma_w|F_o|^2]^{1/2\theta}$.

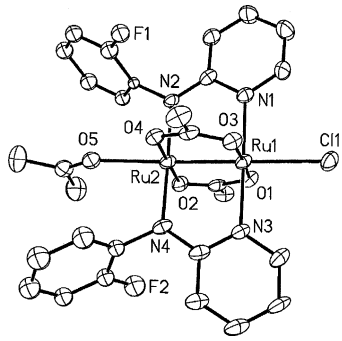

Figure 1. ORTEP diagram of $Ru_2(CH_3CO_2)_2(Fap)_2Cl(ace)$. Hydrogen atoms have been omitted for clarity.

to monitor instrument and crystal stability and the maximum correction on *I* was <1%. The data were integrated using the Siemens SAINT program, with the intensities corrected for Lorentz factor, polarization, air absorption, and absorption due to variation in the path length through the detector faceplate. A psi scan absorption correction was applied based on the entire data set. Redundant reflections were averaged. Final cell constants were refined using 6146 reflections having $I > 10\backslash s(I)$, and these, along with other information pertinent to data collection and refinement, are listed in Table 1. The Laue symmetry was determined to be 2/*m*, and from the systematic absences noted the space group was shown to be either *Cc* or *C*2/*c*. Both fluorophenyl rings were found to be disordered over two orientations, and this was treated using ideal rigid body models. Additionally, one of the orientations has the fluorine disordered between the two ortho positions. A molecule of acetone solvent is present in the lattice, also disordered over two main orientations. All structural parameters and crystallographic data of **2** are described in Table 1.

(25) Bino, A.; Cotton, F. A.; Felthouse, T. R. *Inorg. Chem.* **1979**, *18*, 2599.

Table 2. Selected Bond Lengths (Å) and Bond Angles (deg) of $Ru_2(CH_3CO_2)_2(Fap)_2Cl(ace)$ **2**

bond length		bond angle	
Ru(1)−Ru(2)	2.2945(7)	Ru(1)−Ru(2)−Cl	178.30(5)
Ru(1)−Cl(1)	2.5328(17)	Ru(1)−Ru(2)−N(2)	90.73(13)
Ru(1)−N(1)	2.093(5)	Ru(2)−Ru(1)−N(1)	89.52(14)
Ru(1)−N(3)	2.111(5)	N(1)−Ru(1)−Ru(2)−N(2)	4.59(19)
Ru(2)−N(2)	2.021(4)	N(3)−Ru(1)−Ru(2)−N(4)	5.45(19)
Ru(2)−N(4)	2.040(5)	Ru(1)−Ru(2)−O(4)	89.73(12)
Ru(1)−O(1)	2.043(4)	Ru(2)−Ru(1)−O(3)	88.41(12)
Ru(1)−O(3)	2.052(4)	O(1)−Ru(1)−Ru(2)−O(2)	4.22(16)
Ru(2)−O(2)	2.035(4)	O(3)−Ru(1)−Ru(2)−O(4)	4.15(15)
Ru(2)−O(4)	2.033(4)		

Results and Discussion

Molecular Structure of $Ru_2(CH_3CO_2)_2(Fap)_2Cl(ace)$ (2). Figure 1 illustrates an ORTEP diagram of $Ru_2(CH_3CO_2)_2(Fap)_2Cl(ace)$ (where ace = axially bound acetone) while selected bond lengths and bond angles of the compound are shown in Table 2. The Ru−Ru bond length is 2.2945(7) Å, a value within the 2.275−2.296 Å range previously observed for diruthenium complexes with 2-anilinopyridinate equatorial ligands.[26] The Ru−N_p and Ru−N_a bond lengths as well as the Ru−Ru−Cl bond angles of **2** are within the range of Ru−N bond lengths and Ru−Ru−Cl bond angles for related $Ru_2(L)_4Cl$ derivatives where L is a substituted anilinopyridine.[26] However, the Ru−Ru−N_p and the Ru−Ru−N_a bond angles are slightly larger in $Ru_2(CH_3CO_2)_2(Fap)_2Cl(ace)$ as compared to those of previously studied related compounds while the N−Ru−Ru-N torsion angles are much smaller than those in $Ru_2(L)_4Cl$ where L = $F_x$ap, x = 1, 2, or 3.[26] The difference in torsion angles is likely attributed to less steric hindrance between Fap^- and $CH_3CO_2^-$ than between two Fap groups on the same compound.

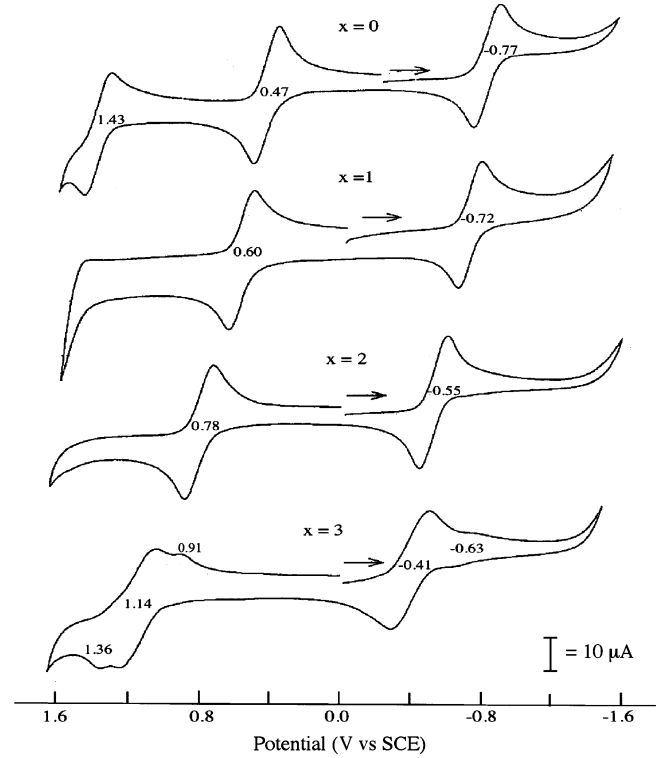

Figure 2. Cyclic voltammograms of $Ru_2(CH_3CO_2)_x(Fap)_{4-x}Cl$ where x = 0−3 in CH_2Cl_2, 0.1 M TBAP. Scan rate is 0.1 V/s.

Table 3. Half-Wave Potentials for $Ru_2^{5+/4+}$ and $Ru_2^{5+/6+}$ Reactions of $Ru_2(CH_3CO_2)_x(Fap)_{4-x}Cl$ in CH_2Cl_2 containing 0.1 M TBAP

# bridging ligand		$Ru_2^{5+/4+}$			$Ru_2^{5+/6+}$		
CH_3CO_2, (x)	Fap	$E_{1/2}$	ΔE_p[a]	i_{pc}/i_{pa}[b]	$E_{1/2}$	ΔE_p[a]	i_{pc}/i_{pa}[b]
3	1	−0.41	180	1.00	1.14	160	1.00
2	2	−0.55	140	0.96	0.78	160	1.08
1	3	−0.72	140	1.00	0.60	140	0.92
0	4	−0.77	160	1.00	0.47[b]	120	1.04

[a] ΔE_p = difference in potential between cathodic and anodic peaks in mV. [b] i_{pc}/i_{pa} = ratio of cathodic (reduction) to anodic (oxidation) peak currents. A theoretical value of 1.0 is expected for a diffusion controlled reaction.

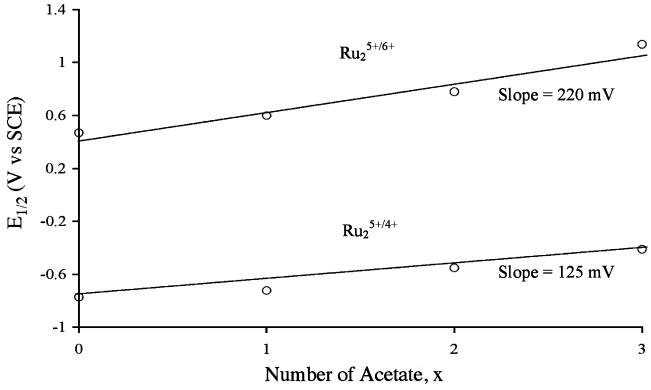

Figure 3. Plot of $E_{1/2}$ vs number of acetate groups (x) on the molecule for $Ru_2^{5+/6+}$ and $Ru_2^{5+/4+}$ reactions of $Ru_2(CH_3CO_2)_x(Fap)_{4-x}Cl$ ($x = 0-3$) in CH_2Cl_2, 0.1 M TBAP.

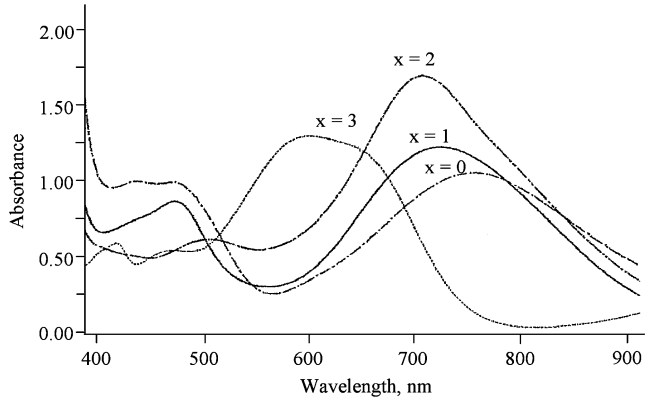

Figure 4. UV−visible spectrum of $Ru_2(CH_3CO_2)_x(Fap)_{4-x}Cl$ ($x = 0-3$) in CH_2Cl_2.

The Ru(1)−Ru(2) bond length of $Ru_2(CH_3CO_2)_2(Fap)_2Cl(ace)$ is 2.2945(7) Å (Table 2), which is 0.014 Å longer than the Ru−Ru bond length of $Ru_2(CH_3CO_2)_4Cl$.[25] It is also 0.09 Å longer than the Ru−Ru bond length of $Ru_2(Fap)_4Cl$, which indicates the lack of a trend in the Ru−Ru bond distance upon replacing $CH_3CO_2^-$ by Fap^-. There was also no evident trend in the Ru−Ru bond length upon replacing $CH_3CO_2^-$ by $admp^-$ in the series of previously characterized $Ru_2(CH_3CO_2)_x(admp)_{4-x}Cl$ derivatives ($x = 0-4$).[4]

The Ru−Cl bond length of $Ru_2(CH_3CO_2)_x(Fap)_{4-x}Cl$ decreases upon replacing the acetate anions by Fap^- and follows the trend $Ru_2(CH_3CO_2)_4Cl$ (2.566 Å) → $Ru_2(CH_3CO_2)_2(Fap)_2Cl(ace)$ (2.5328 Å) → $Ru_2(Fap)_4Cl$ (2.4611 Å) which parallels the lability of the axial Cl^-, as shown by mass spectrometry (Figure S1, Supporting Information) where the molecular ion peak is strongest for the compound with four Fap^- ligands (cpd **0**) and weakest for the one with a single Fap^- bridging ligand (cpd **3**).

Electrochemistry. Cyclic voltammograms of the investigated compounds in CH_2Cl_2, containing 0.1 M TBAP are shown in Figure 2 while half-wave or peak potentials for each redox reaction are given in Table 3 (CH_2Cl_2) and S2 (PhCN and MeCN). Reversible one-electron reductions and oxidations are observed in dichloromethane for the derivatives with two or fewer acetate groups, but a more complex electrochemical behavior occurs for $Ru_2(CH_3CO_2)_3(Fap)Cl$ due to multiple equilibria involving different forms of the axially ligated chloride. This is discussed in a following section of the manuscript.

A linear relationship exists between $E_{1/2}$ and the number of acetate ligands on the diruthenium core for both reduction and oxidation of $Ru_2(CH_3CO_2)_x(Fap)_{4-x}Cl$ (see Figure 3). Plots of $E_{1/2}$ for $Ru_2^{5+/6+}$ and $Ru_2^{5+/4+}$ process vs the number of acetate groups on $Ru_2(CH_3CO_2)_x(Fap)_{4-x}Cl$ ($x = 0-3$) have slopes of 220 mV for oxidation and 125 mV for reduction. Because the slopes of the two correlations in Figure 3 are not identical, the potential gap between the $Ru_2^{5+/4+}$ and $Ru_2^{5+/6+}$ redox couples increases from 1240 mV for the cpd **4** Fap bridging ligands to 1550 mV for the one with only a single Fap ligand (cpd **3**).

UV−Visible Spectroscopy. Figure 4 displays the UV−visible spectrum of $Ru_2(CH_3CO_2)_x(Fap)_{4-x}Cl$ ($x = 0-3$) in CH_2Cl_2 and a summary of the spectral data for the Ru_2^{6+}, Ru_2^{5+}, and Ru_2^{4+} forms of the compounds are given in Table 4. The

Table 4. UV−vis Spectral Data of $Ru_2(CH_3CO_2)_x(Fap)_{4-x}Cl$ where $x = 0-3$ Before and After a One-Electron Reduction or Oxidation in CH_2Cl_2, 0.1 M TBAP

	# bridging ligands						
oxidn state	CH_3CO_2, (x)	Fap	λ_{max}, nm (log ε, M^{-1} cm^{-1})				
Ru_2^{5+}	3	1	415 (3.08)	464 (3.05)	581 (3.35)	643 (3.30)[a]	990 (2.59)
	2	2	431 (3.22)	513 (3.24)		682 (3.62)	
	1	3	429 (3.45)	469 (3.48)		728 (3.51)	
	0[b]	4[b]	428 (3.56)	463 (3.55)		750 (3.58)	
Ru_2^{4+}	3	1	415 (3.11)				
	2	2	469 (3.32)				
	1	3	469 (3.47)				
	0[b]	4[b]	482				
Ru_2^{6+}	3	1	464 (3.27)			640 (3.47)	990 (2.93)
	2	2	433 (3.38)			806 (3.95)	
	1	3	493 (3.44)			898 (3.71)	
	0[b]	4[b]	431 (3.61)			960 (3.71)	

[a] Shoulder at 581 nm band. [b] Ref 26.

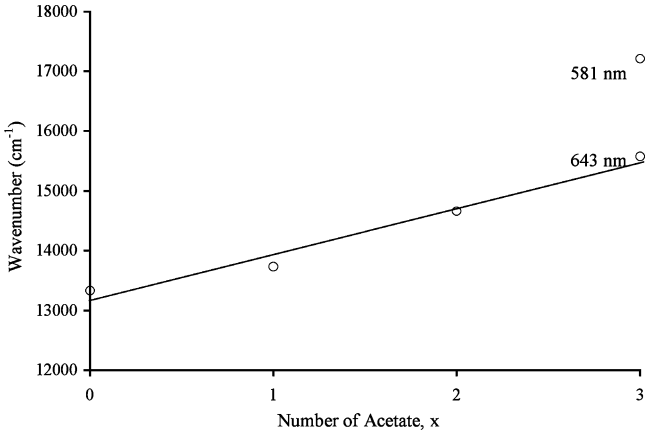

Figure 5. Plot of wavenumber vs number of acetate groups (x) on $Ru_2(CH_3CO_2)_x(Fap)_{4-x}Cl$ for the low-energy absorption band in CH_2Cl_2 (see exact values in Table 4).

initial compound prior to oxidation or reduction of each Ru_2^{5+} species exhibits a low-energy absorption at 581−750 nm and a less intense band at 415−513 nm. Compound **3**, $Ru_2(CH_3CO_2)_3(Fap)Cl$, has an additional band at 990 nm as seen in the table. A band in the range of 580−800 nm for related Ru_2^{5+} compounds was previously attributed[1] to an allowed charge-transfer transition π (ligand, metal) → π^* (Ru_2) or δ^* (Ru_2) transitions and a similar assignment is proposed for compounds in the presently investigated series. An intense band in this range of wavelengths was reported for $Ru_2(F_xap)_4Cl$ where $x = 1$, 2, 3, or 5 and was shown to be sensitive to the type of bridging ligand coordinated to the diruthenium core.[26] This is also the case for the presently investigated compounds where the major visible band of the compound red-shifts upon going from $Ru_2(CH_3CO_2)_3(Fap)Cl$ ($x = 3$) to $Ru_2(Fap)_4Cl$ ($x = 0$) as seen in Figure 4.

Compounds **0**, **1**, and **2** which have an absorption at 682−750 nm differ from $Ru_2(CH_3CO_2)_3(Fap)$ **3** which has a split band at 581 and 643 nm as well as a weak absorption at 990 nm. The 990 nm band of $Ru_2(CH_3CO_2)_3(Fap)Cl$ resembles a near-IR band of $Ru_2(O_2CPr)_4Cl$ (Pr = a propyl group) in CH_3OH which was assigned to an allowed $\delta \rightarrow \delta^*$ transition.[27] A linear correlation exists between the low energy band of compounds **0**−**3** (in cm^{-1}) and the number of acetate ligands on the Ru_2^{5+} unit (Figure 5) when the shoulder at 643 nm is used for the correlation instead of the 581 nm maxima in the case of $Ru_2(CH_3CO_2)_3(Fap)Cl$. This suggests that the 581 nm band might be assigned to a different form of the compound in solution. UV−visible spectra were also obtained for the Ru_2^{4+} and Ru_2^{6+} forms of the compounds after reduction or oxidation in a thin-layer cell and these spectral data are given in Table 4.

UV−visible spectral changes for the $Ru_2^{5+/4+}$ process of each compound upon application of a reducing potential are illustrated in Figure 6a. The intense visible band of Ru_2^{5+} collapses as the reduction proceeds and the final Ru_2^{4+} product exhibits an absorption band at 415−469 nm. This result parallels what has been reported upon reduction of $Ru_2(F_xap)_4Cl$ (where $x = 1$ to 5) under similar solutions conditions (see Table 4).[26] The Ru_2^{4+} form of $Ru_2(Fap)_4Cl$ possess two unpaired electrons[28] and this is also the case for the Ru_2^{4+} form of each examined derivative on the basis of their room temperature magnetic moments which range from 2.92 to 3.33 μB (see Experimental Section).

UV−visible spectral changes during the $Ru_2^{5+/6+}$ process of the compounds with 1−3 acetate bridging ligands are illustrated in Figure 6b. The oxidations of $Ru_2(CH_3CO_2)_2(Fap)_2Cl$ **2** and $Ru_2(CH_3CO_2)(Fap)_3Cl$ **1** to give

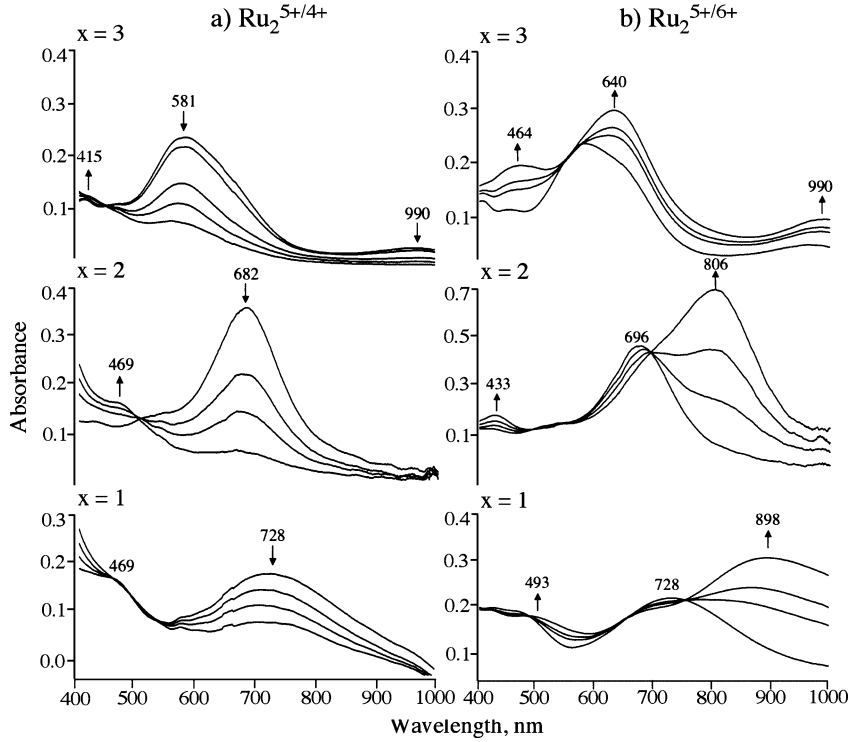

Figure 6. UV−visible spectral changes for the (a) $Ru_2^{5+/4+}$ and (b) $Ru_2^{5+/6+}$ process of $Ru_2(CH_3CO_2)_x(Fap)_{4-x}Cl$ where ($x = 1-3$) upon application of a reducing (part a) or oxidizing (part b) potential in CH_2Cl_2, 0.2 M TBAP.

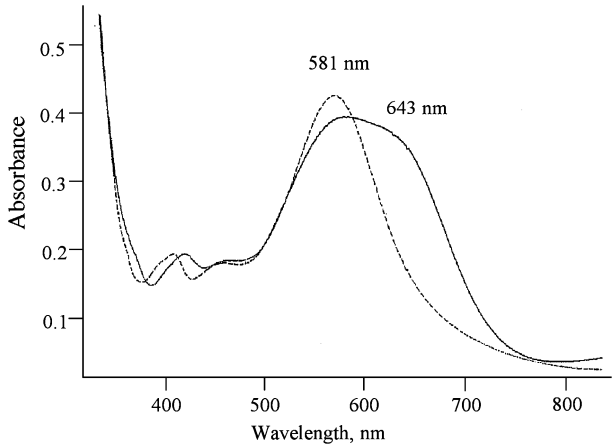

Figure 7. UV−visible spectrum of $Ru_2(CH_3CO_2)_3(Fap)Cl$ **3** in CH_2Cl_2 before (—) and after (---) addition of 0.1 M TBACl.

the Ru_2^{6+} species leads to a spectrum with a more intense absorption band at 806 or 898 nm which is red-shifted from the initial λ_{max} at 682 or 728 nm. These spectral changes resemble what has been reported for the $Ru_2^{5+/6+}$ process of $Ru_2(Fap)_4Cl$ and other diruthenium complexes with similar bridging ligands where the oxidation was assigned as involving removal of an electron from the δ^* orbital.[26]

Interestingly, a different spectral pattern is seen for the $Ru_2^{5+/6+}$ process of $Ru_2(CH_3CO_2)_3(Fap)Cl$ **3**. In this case, the 581 nm band collapses during oxidation while a band at 640 nm increases in intensity (Figure 6b). The initial 990 nm band for compound **3** increases; however, no major low-energy absorption is seen for the oxidized compound as in the case of $Ru_2(CH_3CO_2)_2(Fap)_2Cl$ **2** or $Ru_2(CH_3CO_2)(Fap)_3Cl$, **1**, perhaps because removal of an electron from $Ru_2(CH_3CO_2)_3(Fap)Cl$ **3** involves the π^* orbital instead of δ^*. Thus, a switch in the orbital ordering between π^* and δ^* might occur upon going from $Ru_2(CH_3CO_2)_3(Fap)Cl$ **3** to $Ru_2(Fap)_4Cl$ **0**.

Reactivity of $Ru_2(CH_3CO_2)_x(Fap)_{4-x}Cl$ with excess Cl^-. Figure 7 illustrates UV−visible spectra of $Ru_2(CH_3CO_2)_3(Fap)$-Cl **3** in CH_2Cl_2 before (—) and after (---) adding 0.1 M TBACl to solution while Figure 8 illustrates cyclic voltammograms of three $Ru_2(CH_3CO_2)_x(Fap)_{4-x}Cl$ derivatives ($x = 0$, 2, and 3) in CH_2Cl_2 containing 0.1 M TBACl. We recently reported[29] that $Ru_2(F_3ap)_4Cl$ (F_3ap = 2,4,6-trifluoroanilinopyridinate anion) can axially bind a second Cl^- to yield $[Ru_2(F_3ap)_4Cl_2]^-$. Based on this report, chloride binding should occur for the presently investigated compounds in the presence of TBACl. This is the case for compounds **2** and **3** since the UV−visible spectra (**2** not shown) and the cyclic voltammograms in Figure 8 change upon adding Cl^- to solution.

Compound **3** in CH_2Cl_2, 0.1 M TBAP (Figure 2) exhibits two reductions (at $E_{1/2}$ −0.41 and −0.63 V) as opposed to a single reduction (at $E_{pc} = -0.80$ V) in CH_2Cl_2 containing 0.1 M TBACl (Figure 8). In contrast, **2** in CH_2Cl_2, 0.1 M TBAP

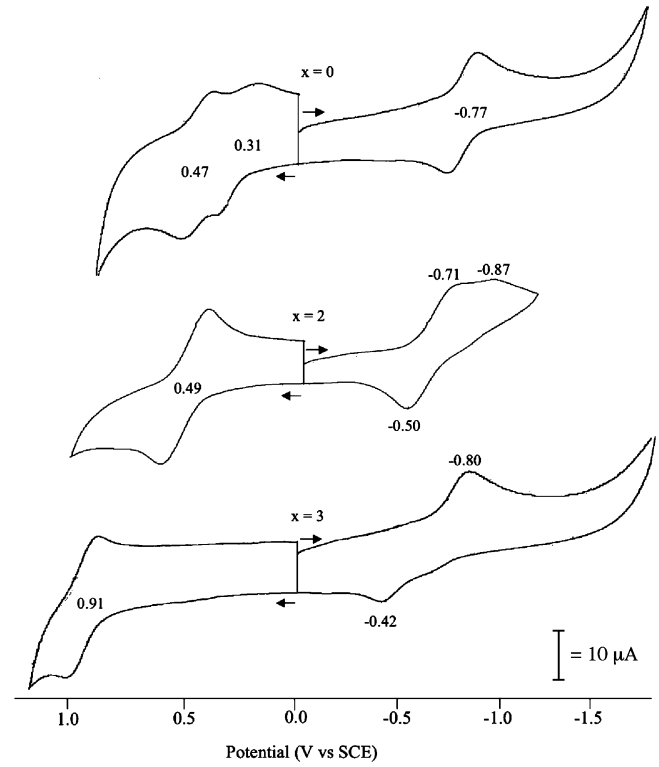

Figure 8. $Ru_2(CH_3CO_2)_x(Fap)_{4-x}Cl$ where $x = 0$, 2, or 3 in CH_2Cl_2, 0.1 M TBACl.

(Figure 2) is characterized by a single reduction at $E_{1/2} = -0.55$ V but exhibits two reductive processes at $E_{pc} = -0.71$ and −0.87 V in CH_2Cl_2 containing 0.1 M TBACl (Figure 8).

In summary the present study shows that $Ru_2(Fap)_4Cl$ and three different mixed-ligand Ru_2^{5+} complexes of the type, $Ru_2(CH_3CO_2)_x(Fap)_{4-x}Cl$ where $x = 1$, 2, or 3 can be synthesized in a single reaction between $Ru_2(CH_3CO_2)_4Cl$ and HFap in refluxing methanol. The derivatives with two or three Fap groups on the molecule exhibit electrochemical and UV−visible spectroscopic behavior quite similar to the diruthenium compound with four Fap ligands. This is not the case for the diruthenium compound with only a single Fap^- bridging ligand, **3**. This difference is attributed to the existence of chemical equilibria involving association and dissociation of the anionic axial ligand on the neutral, reduced and/or oxidized forms of $Ru_2(CH_3CO_2)_3(Fap)Cl$.

Acknowledgment. The support of the Robert A. Welch Foundation (J.L.B., Grant E-918; K.M.K., Grant E-680) is gratefully acknowledged. R.G. also thanks Rice-Houston AGEP for support. T.P. acknowledges support from a TSU Seed Grant and a Departmental Welch Grant. We also thank Dr. J. D. Korp for X-ray analysis.

Supporting Information Available: X-ray crystallographic data for compound **2** (CIF format), mass spectral data of $Ru_2(CH_3CO_2)_x(Fap)_{4-x}Cl$ ($x = 0$, 1, 2, or 3), and a list of redox potentials for the investigated series in PhCN and MeCN. The material is available free of charge via the Internet at http://pubs.acs.org.

IC8017369

(26) Kadish, K. M.; Wang, L.-L.; Thuriere, A.; Van Caemelbecke, E.; Bear, J. L. *Inorg. Chem.* **2003**, *42*, 834.
(27) Miskowski, V. M.; Gray, H. B. *Inorg. Chem.* **1988**, *27*, 2501.
(28) Kadish, K. M.; Wang, L.-L.; Thuriere, A.; Giribabu, L.; Garcia, R.; Van Caemelbecke, E.; Bear, J. L. *Inorg. Chem.* **2003**, *42*, 8309.
(29) Nguyen, M.; Phan, T.; Van Caemelbecke, E.; Kajonkijya, W.; Bear, J. L.; Kadish, K. M. *Inorg. Chem.* **2008**, *47*, 7775.